Precision degrader-antibody conjugates (pDACs) with a SMARCA2/4 dual payload as targeted therapeutics for acute myeloid leukemia

Ryan Holmes[1], Andrew Moore[1], Max Foroutan[1], Jake Karwoski[1], Alex Grego[1], Carly Bachner[1], Neha Bhagawat[1], Corey Basch[1], Soham Maity[1,2], Chun Chen[1], Sarah B. Pawley[1], Vijay Devannah[1], Sina Rezazadeh[1], Ross Kuskovsky[1], Joseph Rager[1], Kenneth Ray[1], Kirsten Gallagher[1], Yue Zou[1], Koichi Ito[1], Diane Heiser[1,3], Sang Hyun Lee[1], Peggy Scherle[1], Andrew P. Combs[1], Andrew W. Buesking[1]

[1]Prelude Therapeutics Incorporated, Wilmington, DE, United States; [2]Current Affiliation: AstraZeneca, Waltham, MA, United States, [3]Current affiliation: Envada, Boulder, CO, United States.

Prelude THERAPEUTICS

A004

Abstract

Degrader payloads offer a compelling opportunity to advance precision medicine through the development of next-generation degrader-antibody conjugates. We have previously described dual SMARCA2/4 degrader payloads that drive potent and selective target degradation, coupled with robust antiproliferative activity across multiple cancer indications. These heterobifunctional molecules were rationally designed to optimize degradation efficiency while maintaining physicochemical properties compatible with antibody drug conjugate (ADC) payload design.

In this work, we report the development of novel LILRB4-targeting x SMARCA2/4 degrader pDACs generated using well-established linker architectures and conjugation strategies. These pDACs demonstrate potent, antigen-dependent activity in acute myeloid leukemia (AML) cell models and selectively kill LILRB4-positive peripheral disease cells in an *ex vivo* assay, providing further validation of our SMARCA2/4 payloads use in pDACs for myeloid cancers.

Precision degrader antibody conjugates (pDACs)

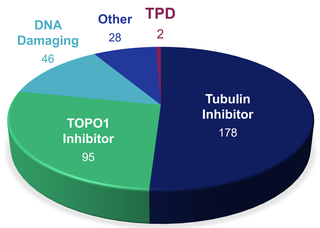

Data source: Morris, J. Beacon ADC by HansonWade. "Analyzing the ADC Boom: Landscape Review." World ADC (San Diego). November 2024. Denotes Payload MOA for clinical stage assets currently in development at time of analysis.

- Most next-gen, clinical ADCs use just three classes of cytotoxic payloads
- Targeted protein degrader (TPD) payloads offer exceptional potency and opportunities for additional benefits of precision
- TPD properties can be designed to limit undesired exposure through clearance and cell-penetration
- TPDs can expand reach of ADCs to cancers and other therapeutic areas beyond traditional cytotoxics

Model of Precision DAC
(DAR 4 example)

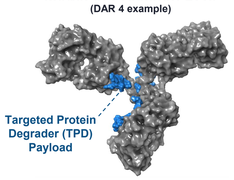

Property	Traditional ADC	Precision DAC
Potency	✓	✓
Antibody selectivity	✓	✓
Payload selectivity	X	✓
PD Marker – payload	X	✓
Non-genotoxic	X	✓

- **Precision DACs enable improved selectivity in two ways[1]**
  - ✓ **Antibodies** target tumor-specific cell surface antigens sparing healthy cells
  - ✓ **Targeted Protein Degraders** address critical proteins in validated biological pathways
- **Potential to deliver both improved efficacy and tolerability[2]**

Next-generation pDACs targeting SWI/SNF complexes

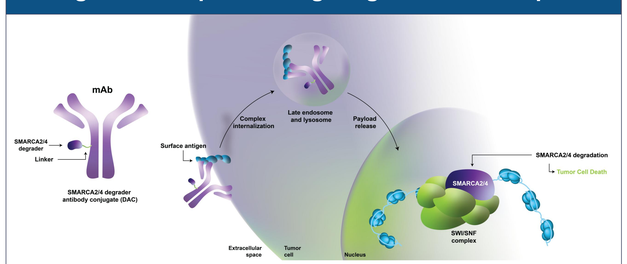

- SMARCA2 (BRM) and SMARCA4 (BRG1) function as the ATP-dependent catalytic subunits of the SWI/SNF complex, facilitating chromatin remodeling and transcriptional regulation[3,4]
- TF/enhancer-driven malignancies, such as prostate cancer, have been shown to rely on the SWI/SNF chromatin remodeling complex for tumor growth and survival[5,6]
- Concurrent inactivation of SMARCA2 and SMARCA4 is poorly tolerated due to the essential role of the SWI/SNF complex in normal tissue homeostasis[7,8]
- Precision degrader antibody conjugates provide the opportunity for deep clinical responses combined with favorable tolerability

Toolbox of SMARCA2/4 dual degrader payloads

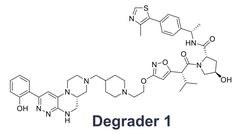

Degrader 1

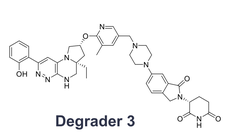

Degrader 3

Degrader	SM2 DC_{50} (D_{max})[a]	SM4 DC_{50} (D_{max})[a]	Fold Selectivity[b]	LNCaP CTG EC_{50} (E_{max})[c]	hPlasma stability $t_{1/2}$ (d)[d]	hLM CL_{int} (mL/min/kg) (%HBF)[e]
1	370 (97%)	2,700 (96%)	7x	210 (96%)	stable	16 (77%)
2	240 (94%)	1,200 (97%)	5x	82 (95%)	stable	19 (90%)
3	40 (97%)	90 (97%)	2x	74 (95%)	1.4	19 (90%)
4	26 (93%)	35 (96%)	1x	49 (94%)	10	17 (79%)

All potency values in pM. [a]HeLa HiBit, 24 h. [b]SMARCA4/SAMRCA2 selectivity ratio. [c]LNCaP CellTiter-Glo, 7-day. [d]Payload incubated in human plasma at 37 °C, 7-day. [e]Human liver microsome stability.

PL01

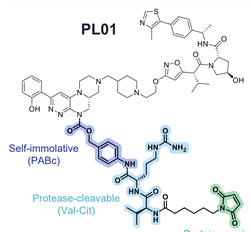

PL03

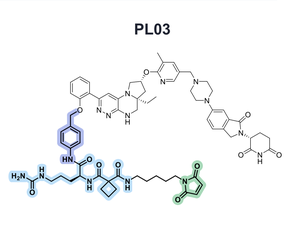

pDAC Descriptors[a]	DAC 01	DAC 02	DAC 03	DAC 04
Payload-linker (PL)	PL01	PL02	PL03	PL04
DAR	3.8	4.0	4.0	3.7
Cellular activity (ng/mL)				
LNCaP SM2 DC_{50} (D_{max})[b]	75 (88%)	42 (85%)	35 (82%)	36 (89%)
LNCaP SM4 DC_{50} D_{max})[b]	2,700 (50%)	300 (66%)	340 (75%)	53 (80%)
LNCaP prolif. EC_{50} (E_{max})[c]	460 (86%)	460 (75%)	7,300 (60%)	210 (82%)
Fold selectivity[d]	>22x	>22x	>1x	>48x

LNCaP (STEAP1+); PC3 (STEAP1-). [a]DACs generated by native cysteine conjugation to anti-STEAP1 mAb, vandortuzumab. [b]LNCaP in-cell western, 24 h. [c]LNCaP CellTiter-Glo, 7-day. [d]Selectivity ratio calculated from PC3/LNCaP CellTiter-Glo assays.

- Anti-STEAP1 SMARCA2/4 pDACs induced robust degradation with all four payloads
- Despite maintaining degradation potency, **DAC 03** failed to elicit antigen-dependent antiproliferative activity

Payload inactivation involves glutarimide hydrolysis

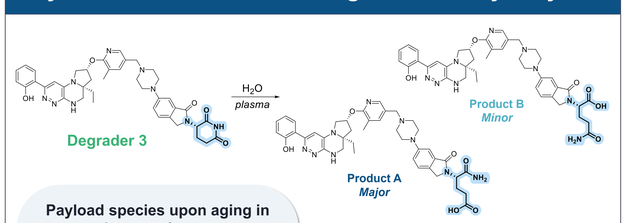

Payload species upon aging in human plasma

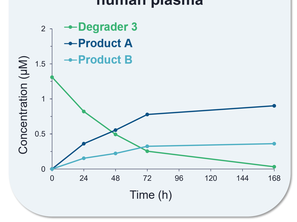

- Two regioisomeric hydrolysis products observed in plasma
- Hydrolysis proceeds to near-quantitative conversion (7 d) and becomes the predominant conjugated species within 2 days[9]
- To advance more potent pDACs, **degrader 4** was developed with improved human plasma stability

LILRB4: A biomarker for AML M4/M5 subtypes

LILRB4 transcript expression across tissue types[10]

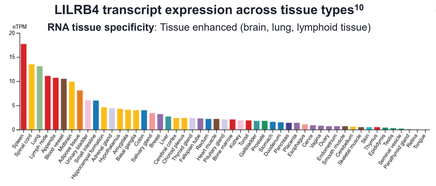

Structure of LILRB4 (ILT3)[11]

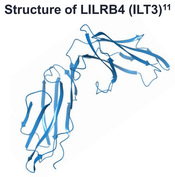

LILRB4 expression in AML[12]

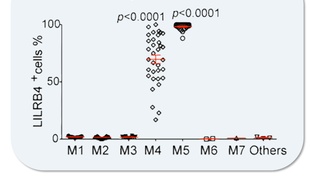

- LILRB4 (ILT3) functions as an inhibitory checkpoint receptor that restrains myeloid cell activation and maintains immune tolerance[12-14]
- LILRB4 is preferentially expressed on monocytic AML blasts, particularly in M4/M5 subtypes, while exhibiting limited expression in non-myeloid tissues, supporting its utility as a biomarker and therapeutic target[12,15]

pDACs demonstrate antigen-dependent activity

EC_{50} in myeloid cell panel

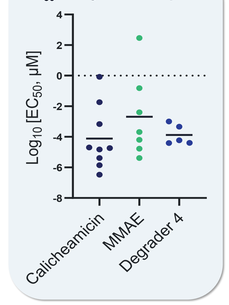

Selective internalization of anti-LILRB4 mAb

Internalization (AUC)[a]	THP-1 (LILRB4 MFI: 175)[b]	KG-1 (LILRB4 MFI: 1)[b]
anti-LILRB4 mAb	33,000	2,500
IgG1 isotype	780	410

THP-1 (LILRB4+); KG-1 (LILRB41-). [a]FabFlour Incucyte, 10 µg/mL. [b]Cell surface binding (LILRB4) measured by FACS.

- Anti-LILRB4 mAb selectively internalizes in LILRB4+ THP-1 cells relative to an isotype control

Myeloid cells respond to SMARCA2/4 degradation

Prolif EC_{50} (pM)[a]	THP-1	KG-1
Degrader 4	1,000	40

THP-1 (LILRB4+); KG-1 (LILRB41-). [a]CellTiter-Glo, 7-day.

- SMARCA2/4 degrader payloads inhibit the growth of myeloid cells comparable to cytotoxic payload calicheamicin

DAC Descriptors[a]	DAC 05	DAC 06	DAC 07
Antibody	anti-LILRB4 mAb	anti-LILRB4 mAb	IgG1 isotype
Payload-linker (PL)	PL04	PL04	PL04
DAR	3.9	5.5	3.9
Cellular activity (ng/mL)			
THP-1 SM2 DC_{50} (D_{max})[b]	<100 (>99%)	<100 (>99%)	*n.t.*
THP-1 SM4 DC_{50} (D_{max})[b]	<100 (>99%)	<100 (>99%)	*n.t.*
THP-1 prolif EC_{50} (E_{max})[c]	92 (52%)	120 (51%)	>10,000 (<1%)
Fold selectivity[d]	>110x	>83x	n/a

THP-1 (LILRB4+); KG-1 (LILRB4-). n.t. = not tested. [a]DACs generated by native cysteine conjugation to fully mouse IgG1 monoclonal antibodies. DAR measured by aHIC and LC-MS. [b]THP-1 Jess Simple Western, 4-pt, 72 h. [c]THP-1 CellTiter-Glo, 7-day. [d]Selectivity ratio calculated from KG-1/THP-1 CellTiter-Glo assays.

- **DAC 05** and **06** exhibit potent, antigen-dependent cellular activity
- Robust selectivity observed compared to the isotype control

Selective targeting of LILRB4+ myeloid cells

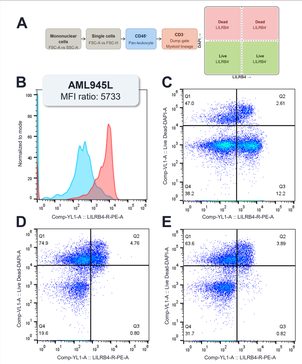

*(A) Flow cytometry gating strategy. (B) Cell surface binding (LILRB4) measured by FACS. (C-E) Flow cytometry plots showing cell death after 7-day treatment of PBMCs isolated from a donor with AML (M4-staging; expressing LILRB4). (C) DMSO. (D) 0.1 µg/mL **DAC 05**. (E) 1.0 µg/mL **DAC 05**.*

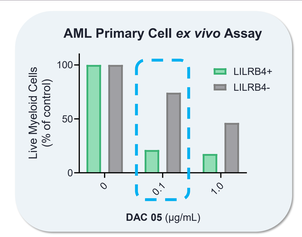

- PBMCs isolated from a patient with LILRB4+ AML (M4-staging) were cultured with **DAC 05** for 7 days.
- Flow cytometric analysis demonstrated dose-dependent depletion of LILRB4+ cells, while sparing LILRB4- cells

Chemistry platform enables reliable synthesis of PL03

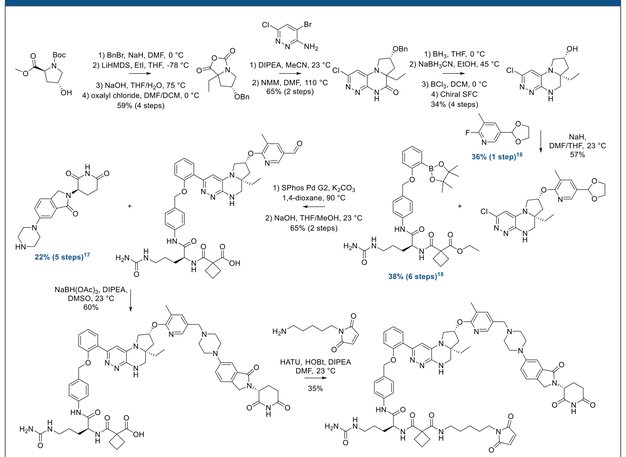

- **PL03** was prepared in 15 steps (LLS)

Conclusions

- Successful pDAC design relies on the coordination of highly potent, stable degrader payloads and antigen selection to address unique modality
- SMARCA2/4 dual degrader demonstrated robust antiproliferative activity in myeloid cell lines, highlighting their potential as next-generation ADC payloads
- Anti-LILRB4 SMARCA2/4 pDACs exhibited potent, antigen-dependent cellular activity *in vitro* and selective activity *ex vivo*, further showcasing the promise of SMARCA2/4 degrader payloads
- These PoC studies provide further validation of our SMARCA2/4 degrader payloads for use in pDACs targeting myeloid diseases

Disclosures

All authors are or were employees of Prelude Therapeutics Incorporated at the time of research and may own equity in the Company.

Acknowledgments

We thank Prelude Therapeutics Inc. for funding this research. We thank Affinity Research Chemicals for their synthetic support.

References

1. Fu, Z., et al. *Sig Transduct Target Ther* **2022**, *7*, 93. **2.** Hong, K. B.; An, H. *J. Med. Chem.* **2023**, *66*, 140. **3.** Gourisankar, S., et al. *Nat Rev Genet.* **2024**, *25*, 340. **4.** Centore, R. C., et al. *Trends Genet.* **2020**, *12*, 936. **5.** Xiao, L., et al. *Nature.* **2022**, *601*, 434. **6.** He, T. et al. *Cancer Cell.* **2024**, *42*, 1336. **7.** Harling, J. D.; Tinworth, C. P. *Nat Commun* **2023**, *14*, 515. **8.** Papillon, J. P. N., et al. *J. Med. Chem.* **2018**, *61*, 10155. **9.** Buesking, A. W. *ACS Spring Meeting*, March 2026. **10.** Leukocyte immunoglobulin-like receptor B4 (LILRB4). https://www.proteinatlas.org (Consensus dataset graph extracted June 2026). **11.** Structure visualized using PDB code 3P2T. **12.** Deng, M., et al. *Nature.* **2018**, *562*, 7728. **13.** Kang, X., et al. *Nat Cell Biol.* **2015**, *5*, 665. **14.** Zheng, J., et al. *Nature* **2012**, *485*, 656. **15.** John, S., et al. *Mol Ther.* **2018**, *26*, 2487. **16.** WO 2025193454. **17.** WO 2022020288. **18.** WO 2025184459